# Normal scaling in globally conserved interface-controlled coarsening of fractal clusters

Avner Peleg,[1] Massimo Conti,[2] and Baruch Meerson[1],*

[1]*Racah Institute of Physics, Hebrew University of Jerusalem, Jerusalem 91904, Israel*
[2]*Dipartimento di Matematica e Fisica, Università di Camerino, and Istituto Nazionale di Fisica della Materia, 62032, Camerino, Italy*
(Received 17 July 2000; revised manuscript received 25 April 2001; published 30 August 2001)

We find that globally conserved interface-controlled coarsening of diffusion-limited aggregates exhibits dynamic scale invariance (DSI) and normal scaling. This is demonstrated by a numerical solution of the Ginzburg–Landau equation with a global conservation law. The general sharp-interface limit of this equation is introduced and reduced to volume preserving motion by mean curvature. A simple example of globally conserved interface-controlled coarsening system: the sublimation/deposition dynamics of a solid and its vapor in a small closed vessel, is presented in detail. The results of the numerical simulations show that the scaled form of the correlation function has a power-law tail accommodating the fractal initial condition. The coarsening length exhibits normal dynamic scaling. A decrease of the cluster radius with time, predicted by DSI, is observed. The difference between global and local conservation is discussed.

Growth of order from disorder in systems with long-range correlations is an intriguing problem which appears in phase ordering [1] and in many other applications. In phase ordering systems, long-range correlations appear most naturally when the system is quenched from the critical temperature $T = T_c$ to $T = 0$. Systems with long-range correlations are often characterizable by fractal geometry [2], and a question arises about the role of the fractal geometry in the coarsening dynamics. Therefore, a lot of attention in different fields of physics has been devoted to a variety of processes of "fractal coarsening" [3–14]. A typical setting for fractal coarsening is the following. At an earlier stage of the dynamics a fractal cluster (FC) develops due to an instability of growth of the "minority phase." Canonical examples are deposition of solute from a supersaturated solution, solidification from an undercooled liquid and viscous fingering in the radial Hele–Shaw cell [2]. When the mass (or heat) source is depleted, fractal coarsening, that is coarsening of fractal clusters by surface tension, becomes dominant. Additional examples appear in the context of sintering [4,7], smoothing of fractal polymer structure in the process of polymer collapse [12], thermal relaxation of rough grain boundaries [14], etc. How does the morphology of the FC change in the process of coarsening? Is there any dynamic scaling behavior, and what are the universality classes?

A major simplifying assumption in an attempt to answer these questions is dynamic scale invariance (DSI). DSI implies that there exists, at late times, a single coarsening length scale $l(t)$ so that the pair correlation function $C(r,t)$ has a self-similar form $g[r/l(t)]$ [1]. Because of the complexity of coarsening systems, DSI has not been proven, except in some simple models [1]. For systems with short-range correlations, there is a lot of evidence supporting DSI from experiments as well as from numerical simulations. The situation is very different for systems with long-range correlations. Toyoki and Honda [3] were the first to apply the DSI hypothesis to such systems, considering systems with non-

conserved order parameter. Particle simulations of nonconserved phase ordering following a quench from $T = T_c$ to $T = 0$ showed that in this case DSI holds, and that new universality classes for the equal-time two point correlation function appear [15]. However, a large discrepancy between the approximate theoretical correlation function and the numerical one still remains unexplained. Implications of (mass) conservation in fractal coarsening were considered more recently [4,8]. Most remarkable of them is the predicted decrease of the cluster radius with time. However, there has been no convincing evidence (neither in experiment, nor in simulations) in favor of DSI in conserved fractal coarsening. Moreover, anomalous scaling and breakdown of DSI were observed in recent simulations of locally conserved edge-diffusion- [7] and bulk-diffusion-controlled [9,10] fractal coarsening. (By definition, normal scaling follows from the governing equations when one assumes DSI. Anomalous scaling may occur when DSI is broken.) We report here our finding that DSI and normal scaling hold in the process of *interface-controlled* fractal coarsening with a *globally* conserved order parameter. This system is apparently the first realistic conserved fractal coarsening system where this simplifying and beautiful concept is found to work.

As we show below, a simple example of globally conserved interface-controlled coarsening is provided by the sublimation/deposition dynamics of a solid and its vapor in a small closed vessel kept at a (constant) temperature below the melting point [16]. Globally conserved interface-controlled coarsening also appears in the growth of solid particles undergoing a chemical reaction in which a gaseous compound is formed [17]. Another example appears in the context of attachment/detachment-controlled nanoscale fluctuations at solid surfaces [18], where it has been found possible to single out the interface-controlled kinetics [19]. There is also a strong empiric evidence in favor of interface-controlled transport during the cluster coarsening in electrostatically driven granular flows [20].

Globally conserved interface-controlled dynamics is also related to a wide range of multiphase coarsening systems. Sire and Majumdar [21] showed that in the large $q$ limit the

───────────
*Email address: meerson@cc.huji.ac.il

dynamics of the $q$-state Potts model (see Ref. [1]) is equivalent to globally conserved interface-controlled dynamics with an area fraction $1/q$. This limit is of special importance. Indeed it is known that in the large $q$ limit the $q$-state Potts model describes correctly some of the main characteristics of the coarsening of polycrystalline materials [22], and of the dynamics of dry soap froths [23].

Here is an outline of the rest of the paper. We shall work with the Ginzburg-Landau equation with a global conservation law (GCL). The corresponding sharp-interface theory is introduced, and an experimental realization of the model is presented in detail. At late times the general sharp-interface theory is reducible to volume preserving motion by mean curvature. Assuming DSI, one can then predict scaling behavior of the correlation function, a decrease of the cluster radius with time and normal scaling of the coarsening length $l(t)$. Our extensive numerical simulations of the coarsening of two-dimensional (2D) diffusion-limited aggregates (DLAs) support all these predictions. We shall conclude by pointing out the main difference between global and local conservation.

We adopt a Ginzburg-Landau free energy functional

$$F[u] = \int [(1/2)(\nabla u)^2 + V(u) + Hu] d^d\mathbf{r}, \qquad (1)$$

where $V(u) = (1/4)(1-u^2)^2$ is a double-well potential, $u(\mathbf{r},t)$ is the order parameter and fluctuations are neglected. The effective "magnetic field" $H = H(t)$ changes in time so as to impose the GCL: $\langle u \rangle = $ const, where $\langle \cdots \rangle$ denotes a spatial average

$$\langle \cdots \rangle = L^{-d} \int (\cdots) d^d\mathbf{r}. \qquad (2)$$

$L$ is the system size and the integration is over the whole system. The dynamics is described by a simple gradient descent

$$\frac{\partial u}{\partial t} = -\frac{\delta F}{\delta u} = \nabla^2 u + u - u^3 - H(t). \qquad (3)$$

Using Eq. (3) and the GCL, one gets $H(t) = \langle u - u^3 \rangle$ (periodic boundary conditions are assumed). Therefore, Eq. (3) is a nonlocal reaction-diffusion equation [24–27]. In the context of phase ordering it can be called the Ginzburg–Landau equation with a GCL. To make theoretical progress, one should work in the sharp-interface limit valid at late times, when the system already consists of large domains of "phase 1" and "phase 2" divided by a thin interface [27]. At this stage $H(t)$ is both small, $H(t) \ll 1$, and slowly varying in time. The phase field in the phases 1 and 2 is uniform and rapidly adjusts to the current value of $H(t)$, so $u = -1 - H(t)/2$ and $1 - H(t)/2$, respectively. For brevity, we will consider the 2D case. The normal velocity of the interface is [27]

$$v_n(s,t) = (3/\sqrt{2})H(t) - \kappa(s,t), \qquad (4)$$

where $s$ is the coordinate along the interface and $\kappa$ is the local curvature of the interface. A positive $v_n$ corresponds to the interface moving toward phase 2, while $\kappa > 0$ when the interface is convex towards phase 2.

An equation for $H(t)$ follows from GCL [27]:

$$\frac{4A(t)}{L^2} - H(t) = \text{const}, \qquad (5)$$

where $A(t) = \int_{u(\mathbf{r},t)>0} d^2\mathbf{r}$ is the cluster area. Equations (4) and (5) make a closed set and provide the sharp-interface formulation to our problem.

Remarkably, this simple sharp-interface model is a good approximation to the following physical process. Consider the sublimation/deposition dynamics of a solid, e.g., an amorphous ice, and its vapor in a small closed vessel kept at a constant temperature. As the acoustic time in the gas phase is short compared to the coarsening time, the gas pressure and density remain uniform in space, changing only in time. This character of mass transport in the vapor phase makes the coarsening dynamics conserved globally rather than locally, which leads to different kinetics. We shall derive the governing equations for the dynamics of this system in three dimensions (3D), and also give the results for 2D. The derivation is based only on a few assumptions which are well accepted at intermediate and late times of a coarsening process.

The net flux of molecules into the solid phase is given by the difference between the outward flux of solid molecules into the vapor phase $J_\Gamma$ and the inward flux of vapor molecules $J_v$

$$J_{net} = n_s v_n = J_\Gamma - J_v, \qquad (6)$$

where $n_s$ is the constant number density of the solid phase. Notice that $J_\Gamma$ is equal to the (inward) flux of vapor molecules in equilibrium with a solid surface with mean curvature $\kappa$. The flux of molecules of an ideal gas *striking* a surface is given by

$$J = n \left( \frac{k_B T}{2\pi m} \right)^{1/2}, \qquad (7)$$

where $n$ is the density, $k_B$ is the Boltzmann constant, $T$ is the temperature, and $m$ is the mass of one molecule. Combining Eqs. (6) and (7) we obtain

$$J_{net} = n_s v_n = \alpha \left( \frac{k_B T}{2\pi m} \right)^{1/2} (n_\Gamma - n_v), \qquad (8)$$

where $n_v = n_v(t)$ is the actual spatially uniform and time-dependent number density of the vapor phase, and $n_\Gamma$ is the density of the vapor in equilibrium with a surface with mean curvature $\kappa$. The coefficient $\alpha$ obeying $0 < \alpha < 1$ accounts for the fact that only a fraction of the impinging vapor molecules indeed goes into the solid phase. The density $n_\Gamma$ is given by the Gibbs–Thomson relation

$$n_\Gamma = n_0(1 - \lambda\kappa), \qquad (9)$$

where $n_0$ is the density of the vapor phase in equilibrium with a flat interface of the solid, $\lambda$ is the capillary length, and the mean curvature $\kappa$ is the sum of the two local principal curvatures. In writing Eq. (9) one assumes that $\lambda \kappa \ll 1$. The minus sign in the last equation is due to our sign convention for $\kappa$: $\kappa > 0$ when the interface is convex towards the solid phase. Substituting Eq. (9) into Eq. (8) and denoting $\Delta n = n_v - n_0$, we arrive at the following expression for $v_n$:

$$v_n = -\frac{\alpha \lambda n_0}{n_s}\left(\frac{k_B T}{2\pi m}\right)^{1/2}\left[\kappa + \frac{\Delta n}{\lambda n_0}\right]. \quad (10)$$

Since the total number of molecules in the system $N_0$ is constant, the *global* conservation law is given by

$$n_s V_s(t) + n_v(t)[L^3 - V_s(t)] = N_0 = \text{const}, \quad (11)$$

where $V_s(t)$ is the total volume occupied by the solid phase and $L$ is the linear size of the vessel. As $n_v(t) \ll n_s$, and assuming that throughout the dynamics $V_s(t) \ll L^3$, the third term on the left hand side of Eq. (11) can be neglected. This leads to

$$\frac{V_s(t)}{L^3} + \frac{\Delta n(t)}{n_s} = \text{const}. \quad (12)$$

For a 2D system $v_n$ is given by an equation similar to Eq. (10), and the global conservation law takes the form

$$\frac{A_s(t)}{L^2} + \frac{\Delta n(t)}{n_s} = \text{const}, \quad (13)$$

with $A_s(t)$ the total area occupied by the solid phase. We see that Eqs. (10) and (13) for the sublimation/deposition dynamics are similar in form to the general globally conserved sharp-interface Eqs. (4) and (5), and these two models can be mapped into each other exactly. Specifically, the role of the magnetic field in the general theory is played by the vapor supersaturation $\Delta n$ in the sublimation/deposition dynamics.

Possible additional examples of globally conserved interface-controlled dynamics obeying Eqs. (10) and (13) are provided by some chemical systems. Consider a solid that can undergo a chemical reaction with a gas in which a gaseous compound is formed. For example: $Pt + O_2 = PtO_2$, where at sufficiently high temperatures $PtO_2$ is a gas, and the reaction takes place at the surface of the solid Pt. Using the same considerations as in the sublimation/deposition example, we obtain exactly the same Eqs. (10) and (13), with $PtO_2$ playing the role of the vapor phase. In fact, Wynblatt and Gjostein considered such dynamics [17], but without setting the conservation law (that is, in an open vessel), and referring only to spherical particles.

Equations (4) and (5) of the general sharp-interface theory can often be further simplified. Compute the cluster area loss rate

$$\dot{A}(t) = \oint v_n(s,t)ds = \Lambda(t)\left[\frac{3}{\sqrt{2}}H(t) - \overline{\kappa(s,t)}\right], \quad (14)$$

where the overbar stands for averaging over the interface

$$\overline{\kappa(s,t)} = \frac{1}{\Lambda(t)}\oint \kappa(s,t)ds \quad (15)$$

and $\Lambda(t)$ is the cluster perimeter. If the cluster area is conserved, then $H(t) = (\sqrt{2}/3)\overline{\kappa(s,t)}$ which yields

$$v_n(s,t) = \overline{\kappa(s,t)} - \kappa(s,t). \quad (16)$$

This is area-preserving motion by curvature (in 2D), or volume-preserving motion by mean curvature (in 3D) [25,27,28]. Dynamics (16) shortens the interface length (in 2D), or area (in 3D) [25,28]. This nonlocal coarsening model is simpler than the better known "Laplacian coarsening model" (derivable from the Cahn–Hilliard equation [1,29]) which describes the late-time asymptotics of the locally conserved, bulk-diffusion-controlled coarsening.

A single circular (in 2D) or spherical (in 3D) domain of one of the phases in the "sea" of the other phase represents the only stable two-phase steady state of model (16) not directly imposed by the system boundaries [25,27]. In this work we investigate the relaxation dynamics which start from complex initial conditions. As always in the phase ordering theory, we are interested in a (very long) time range when, on one hand, irrelevant details of the initial conditions are forgotten but, on the other hand, the system is still very far from the simple final state. It is this intermediate time range where one can expect dynamic scaling behavior [1]. Assuming DSI, we can estimate the interface velocity as $v_n \sim dl/dt$. Each of the terms on the right side of Eq. (16) is of order $1/l$ (except for critical quench, when the first term averages to zero). Equating and integrating yields the normal scaling: $l(t) \sim t^{1/2}$. Therefore, GCL does not change the dynamic scaling. The same result (again, when assuming DSI) follows from dynamic renormalization group arguments applied to Eq. (3) (with a Gaussian white noise term) [30]. For short-range correlations this result was supported by kinetic Monte Carlo simulations of critical [31] and off-critical [21] quench, and by a numerical solution of Eq. (3) for both critical, and off-critical quench [32]. For critical quench, the coarsening morphology is that of interpenetrating domains, while for off-critical quench it is that of Ostwald ripening.

Let us return to fractal coarsening. The initial conditions are FCs characterizable by fractal dimension $D$ on an interval of scales between the lower and upper cutoffs $\tilde{l}_0$ and $\tilde{L}_0$. The DSI-based coarsening scenario [3,4,8] assumes that the fractal dimension of the cluster remains constant on a shrinking interval of distances between the lower cutoff $l(t)$ (the coarsening length), and an upper cutoff $\tilde{L}(t)$. Now, the perimeter $\Lambda$ and area $A$ of the FC can be estimated as [2]

$$\Lambda \sim l(\tilde{L}/l)^D \quad \text{and} \quad A \sim l^2(\tilde{L}/l)^D, \quad (17)$$

respectively. Area conservation yields $\tilde{L} \sim l^{(D-2)/D} \sim t^{-(2-D)/2D}$ (the characteristic radius of the FC decreases with time) [4,8]. This follows $\Lambda(t) \sim l^{-1}(t) \sim t^{-1/2}$. One can also predict the asymptotic shape of the equal-time pair correlation function at large times: $C(r,t) \to g[r/l(t)]$. At dis-
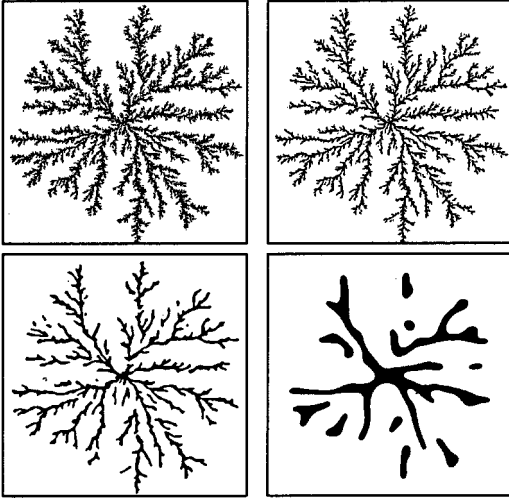
FIG. 1. Evolution of a DLA cluster undergoing an interface-controlled coarsening in a globally conserved system. The upper row corresponds to $t=0$ (left) and 12.6 (right), the lower row to $t=126.4$ (left) and 1856.6 (right).



FIG. 2. Scaling form of the correlation function $C(r,t)$ for time moments $t=400.0,\ 587.0,\ 1264.8$ and 1856.6. The inset shows the same data on a log-log plot. The solid line, serving as a reference, represents a power-law with an exponent $D-2=-0.25$.

tances $r \ll l(t)$ from a typical reference point inside the cluster the correlation function should obey the Porod law: $g(\xi)=1-k\xi$ with a constant $k$ of order unity. At $l(t) \ll r \ll \tilde{L}(t)$ we have $g(\xi) \sim \xi^{D-2}$ (see Ref. [8]), a power-law tail with the same exponent as in $C(r,t=0)$. Finally, the duration of the fractal coarsening stage should scale like the cluster area $A$. This estimate follows from the fact that, by the end of this stage, the lower and upper cutoffs of the fractal cluster become comparable.

In order to check these predictions, we solved Eq. (3) numerically on a domain $2048 \times 2048$ with no flux (that is, zero normal component of $\nabla u$) at the boundary. The accuracy of the numerical scheme was monitored by checking the (approximate) conservation law (5) which was found to hold with an accuracy better than 0.2% for $t>3$.

We used ten different DLA clusters [33] as the initial conditions. This choice makes it possible to compare the interface-controlled fractal coarsening with bulk-diffusion-controlled coarsening, where anomalous scaling and breakdown of DSI were observed for DLA clusters [9,10]. To prevent fragmentation at an early stage of coarsening, the clusters were reinforced by an addition of peripheral sites, similar to Ref. [5]. The average fractal dimension of these clusters, determined from the correlation function (18), was 1.75.

Introducing the density $\rho(\mathbf{r},t)=(1/2)[u(\mathbf{r},t)+1]$, we identify the cluster as the locus where $\rho(\mathbf{r},t) \geqslant 1/2$. Snapshots of the coarsening process are shown in Fig. 1. One can see that larger features grow at the expense of smaller ones. At late times the cluster radius decreases, as predicted by DSI. The predicted "shrinking exponent" $(D-2)/(2D) \simeq -0.07$ is too small to be measured accurately. A similar decrease of the cluster size is evident in the pictures obtained in kinetic Monte Carlo simulations of area-preserving interface-controlled coarsening of DLA clusters [6], although the authors of Ref. [6] did not comment on it.

To characterize the dynamics, several quantities were sampled and averaged over the ten initial conditions:
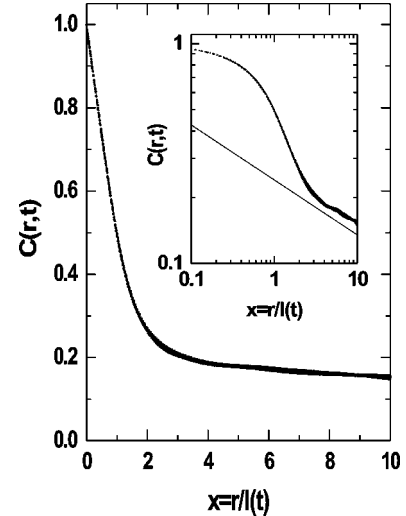
(1) The cluster area.

(2) The (circularly averaged) correlation function, normalized at $r=0$.

$$C(r,t)=\frac{\langle \rho(\mathbf{r}'+\mathbf{r},t)\rho(\mathbf{r}',t)\rangle}{\langle \rho^2(\mathbf{r}',t)\rangle}. \qquad (18)$$

(3) The coarsening length scale $l(t)$, computed from equation $C(l,t)=1/2$.

(4) The cluster perimeter $\Lambda(t)$ computed by a standard algorithm [34].

The cluster area was found to be constant with an accuracy better than 0.5% for $t>10$, and better than 0.15% for $t>100$. Hence, area preserving motion by curvature, Eq. (16), provides an accurate description to this regime. Figure 2 shows that, at late times ($t>100$), $C(r,t)$ approaches a scaled form. The scaled function has a long-range power-law tail with an exponent $D-2$ (the same as in the initial condition), see the inset of Fig. 2. Noticeable is the absence of any additional dynamic length scales, in a striking contrast to the locally conserved fractal coarsening [10]. The dynamics of $l(t)$ is shown in Fig. 3 together with the pure $t^{1/2}$ power-law line (serving as a reference for the expected late-time behavior) and a corrected power-law fit $l(t)=l_0+bt^{\alpha}$ with $\alpha=0.49,\ b=1.2$ and $l_0=5.0$.

Figure 3 shows that convergence of $l(t)$ to scaling is relatively slow in comparison with the cases of critical and off-critical quench [32]. Therefore we show, in Fig. 4, a different method [35] of determining the dynamic exponent, suitable for a slow convergence. In this method one defines a (time-dependent) effective exponent: $\alpha_0(t)=d\ln l(t)/d\ln t$. Under the normal scaling assumption, one can determine the "true" dynamic exponent by plotting $\alpha_0(t)$ vs $l^{-1}(t)$ and extrapolating it to $t \to \infty$, that is to $l^{-1}(t) \to 0$, where corrections to scaling due to subleading terms are negligible. The values of
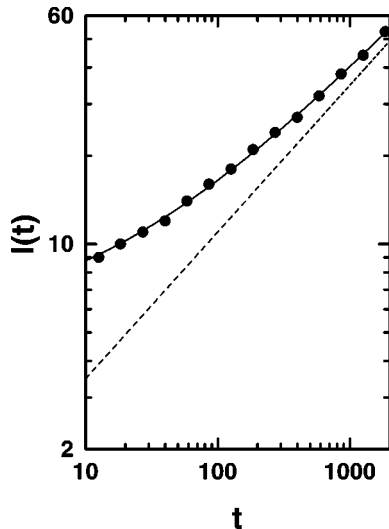
FIG. 3. The coarsening length $l(t)$ vs time (circles). The solid line is a corrected power-law fit: $l(t) = l_0 + bt^\alpha$ with $\alpha = 0.49$, $l_0 = 5.0$, and $b = 1.2$. The dotted line represents a pure $t^{1/2}$ power law.



FIG. 4. The time-dependent effective dynamic exponent $\alpha_0(t)$ versus $1/l(t)$. The solid line is a linear fit.

$\alpha_0(t)$ are computed from $\alpha_0(t) = \log_{10}[l(10t)/l(t)]$. This procedure yields $\alpha = 0.50$, that is $l(t)$ exhibits normal scaling.

The same procedures were used for an analysis of the dynamic behavior of the cluster perimeter $\Lambda(t)$. We found the same normal scaling: $\Lambda^{-1}(t) \sim t^{1/2}$. Irisawa et al. [6] reported an exponent 0.38 for $\Lambda^{-1}(t)$ in their kinetic Monte Carlo simulations. Their graph shows, however, an increase of the effective exponent at late times. We believe that a careful analysis of their data would also lead to an exponent of 1/2.

Thus, all predictions following from the DSI hypothesis: the normal scaling of $l(t)$, a decrease of the characteristic radius of the FC with time and scaling behavior of the correlation function (including its power-law tail), are confirmed by numerical simulations. We therefore conclude that globally conserved interface-controlled coarsening of DLA clusters exhibits DSI and normal scaling. This behavior stands in contrast to the breakdown of scale invariance observed in diffusion-controlled coarsening of DLA clusters [9,10], where the order parameter was conserved *locally*. The mechanism of scaling violations in locally conserved systems is not known at present, therefore a comparison be-

tween the two systems is instructive. We notice that global transport, characteristic for interface-controlled systems, is uninhibited by Laplacian screening effects typical for locally conserved systems. In other words, large-scale dynamics is not suppressed in globally conserved systems, in contrast to locally conserved ones. This difference is observed already in a simpler setting of an area-preserving relaxation of a long slender bar. In the locally conserved case the bar acquires a dumbbell shape, while its initial width remains (almost) constant and represents a relevant length scale until late times [10]. On the contrary, in the globally conserved case a bar develops a fingerlike shape, and its dimensions are changing on the same time scale [36].

We should emphasize that at present we are not aware of any experiment where interface-controlled coarsening of *fractal clusters* was observed. By contrast, there are many experimental situations where coarsening of fractal clusters occurs in locally conserved (bulk diffusion-controlled) systems [9]. Our choice of the initial conditions has enabled us to investigate fractal coarsening in a conserved system but without the Laplacian screening effects. This helped us to single out the reason for scaling violations observed in the fractal coarsening of locally conserved systems.

[1] A. J. Bray, Adv. Phys. **43**, 357 (1994).

[2] J. Feder, *Fractals* (Plenum, New York, 1988); T. Vicsek, *Fractal Growth Phenomena* (World Scientific, Singapore, 1992); P. Meakin, *Fractals, Scaling and Growth Far from Equilibrium* (Cambridge University Press, Cambridge, 1997).

[3] H. Toyoki and K. Honda, Phys. Lett. **111A**, 367 (1985).

[4] R. Sempéré, D. Bourret, T. Woignier, J. Phalippou, and R. Jullien, Phys. Rev. Lett. **71**, 3307 (1993).

[5] T. Irisawa, M. Uwaha, and Y. Saito, Europhys. Lett. **30**, 139 (1995).

[6] T. Irisawa, M. Uwaha, and Y. Saito, Fractals **4**, 251 (1996).

[7] N. Olivi-Tran, R. Thouy, and R. Jullien, J. Phys. I **6**, 557 (1996).

[8] B. Meerson and P. V. Sasorov, e-print cond-mat/9708036.

[9] M. Conti, B. Meerson, and P. V. Sasorov, Phys. Rev. Lett. **80**, 4693 (1998).

[10] M. Conti, B. Meerson, and P. V. Sasorov, e-print cond-mat/9912426.

[11] A. Peleg and B. Meerson, Phys. Rev. E **59**, 1238 (1999); **62**, 1764 (2000).

[12] G. E. Crooks, B. Ostrovsky, and Y. Bar-Yam, Phys. Rev. E **60**, 4559 (1999).

[13] S. V. Kalinin *et al.*, Phys. Rev. E **61**, 1189 (2000).

[14] P. Streitenberger, in *Paradigms of Complexity. Fractals and Structures in Sciences*, edited by M. N. Novak (World Scientific, Singapore, 2000), p. 135.

[15] K. Humayun and A. J. Bray, J. Phys. A **24**, 1915 (1991); Phys. Rev. B **46**, 10 594 (1992).

[16] One can observe an uncontrolled version of this phenomenon while looking at slowly changing ice patterns on the double window of an airplane flying at a high altitude.

[17] P. Wynblatt and N. A. Gjostein, in *Progress in Solid State Chemistry*, edited by J. O. McCaldin and G. Somojrai (Pergamon, Oxford, 1975), Vol. 9, p. 21.

[18] M. Zinke-Allmang, L. C. Feldman, and M. H. Grabow, Surf. Sci. Rep. **16**, 277 (1992).

[19] Z. Toroczkai and E. Williams, Phys. Today **52** (12), 24 (1999).

[20] I. S. Aranson *et al.*, Phys. Rev. Lett. **84**, 3306 (2000).

[21] C. Sire and S. N. Majumdar, Phys. Rev. Lett. **74**, 4321 (1995); Phys. Rev. E **52**, 244 (1995).

[22] G. S. Grest, M. P. Anderson, and D. J. Srolovitz, Phys. Rev. B **38**, 4752 (1988).

[23] J. A. Glazier, M. P. Anderson, and G. S. Grest, Philos. Mag. B **62**, 615 (1990).

[24] L. Schimansky-Geier, Ch. Zülicke, and E. Schöll, Z. Phys. B: Condens. Matter **84**, 433 (1991).

[25] J. Rubinstein and P. Sternberg, IMA J. Appl. Math. **48**, 249 (1992).

[26] A. S. Mikhailov, *Foundations of Synergetics I. Distributed Active Systems* (Springer, Berlin, 1993).

[27] B. Meerson and P. V. Sasorov, Phys. Rev. E **53**, 3491 (1996).

[28] M. Gage, Contemp. Math. **51**, 51 (1986).

[29] R. L. Pego, Proc. R. Soc. London, Ser. A **422**, 261 (1989).

[30] A. J. Bray, Phys. Rev. Lett. **66**, 2048 (1991), and references therein.

[31] J. F. Annett and J. R. Banavar, Phys. Rev. Lett. **68**, 2941 (1992); L. L. Moseley, P. W. Gibbs, and N. Jan, J. Stat. Phys. **67**, 813 (1992); A. D. Rutenberg, Phys. Rev. E **54**, 972 (1996).

[32] M. Conti, B. Meerson, A. Peleg, and P. V. Sasorov (unpublished).

[33] T. A. Witten and L. M. Sander, Phys. Rev. Lett. **47**, 1400 (1981).

[34] J. R. Parker, *Practical Computer Vision Using C* (Wiley, New York, 1993), p. 51.

[35] D. A. Huse, Phys. Rev. B **34**, 7845 (1986).

[36] A. Peleg, B. Meerson, A. Vilenkin, and M. Conti, Phys. Rev. E **63**, 066101 (2001).